A Comparative Study on the Self-Assembly of an Amyloid-Like Peptide at Water–Solid Interfaces and in Bulk Solutions

QIQIGE DU,[1,2] BIN DAI,[2] JIAHUA HOU,[1] JUN HU,[2] FENG ZHANG,[1]* AND YI ZHANG[2]*
[1]*School of Life Sciences, Inner Mongolia Agricultural University, Hohhot 010018, China*
[2]*Key Laboratory of Interfacial Physics and Technology, Shanghai Institute of Applied Physics, Chinese Academy of Sciences, Shanghai 201800, China*

KEY WORDS self-assembly; amyloid peptide; interface; atomic force microscopy

Abstract In the past years the self-assembly of amyloid-like peptides has attracted increasing attentions, because it is highly related to neurodegenerative diseases and has a potential for serving as nanomaterial to fabricate novel and useful nanostructures. In this paper, we focused on the role of interfacial conditions in the self-assembly of an amyloid-like peptide, termed Pep11. It was found that, when dissolved in bulk solutions, Pep11 formed into β-sheet structures and assembled into long filaments in several hours, as revealed by Thioflavin T fluorescence and transmission electron microscopy (TEM) morphology characterization, respectively. When the peptide solution was added onto a mica/HOPG substrate, peptide filaments with three preferred orientations with an angle of 60° to each other were formed immediately, as imaged in situ by atomic force microscopy (AFM). However, the kinetics in filament formation and the morphologies of the formed beta sheet either on HOPG and mica or in bulk solutions were quite different. These results indicate that the interfacial properties dramatically affect the peptide self-assembly process. *Microsc. Res. Tech. 78:375–381, 2015.*

INTRODUCTION

Recently, amyloid fibrils of peptides and proteins have attracted considerable research attentions because these structures are not only highly related to a number of progressive neurodegenerative diseases (Butterfield and Lashuel, 2010; Chiti and Dobson, 2006; Murphy, 2007), but also have shown great potential in serving as nanomaterials for applications in *de novo* nanodevice design and fabrication (Bittner, 2005; Cherny and Gazit, 2008; Knowles and Buehler, 2011; Lashuel et al., 2000; Reches and Gazit, 2003; Ryadnov et al., 2003; Vauthey et al., 2002; Wagner et al., 2005), scaffolds of tissue (Ellis-Behnke et al., 2006; Yokoi et al., 2005), drug delivery (Lim et al., 2007), biosensors (Yang et al., 2009; Yemini et al., 2005), retroviral gene transfer (Yolamanova et al., 2013), carbon dioxide capture (Li et al., 2014), and catalysis (Rufo et al., 2014).

Surface assisted self-assembly of amyloid-like peptides is particularly interesting since the supporting substrate often plays the most important role in controlling both the morphologies and kinetics of the adsorbed assembly (Brown et al., 2002; Ha and Park, 2005; Hoyer et al., 2004; Kowalewski and Holtzman, 1999; Mao et al., 2011; Zhu et al., 2002). For example, we have reported the substrate assisted self-assembly of an amyloid-related hydrophobic peptide, GAV-9 (NH_2-VGGAVVAGV-$CONH_2$), a conserved sequence of some neurodegenerative-disease-related proteins (Du et al., 2003). The in situ atomic force microscopy (AFM) as well as all-atom molecular dynamics (MD) (Kang et al., 2013) simulations showed epitaxial growth of GAV-9 on both hydrophilic mica and hydrophobic highly oriented pyrolytic graphite (HOPG), however, with different morphologies and molecular arrangements. Studies carried out by other groups also indicated that the Alzheimer's disease-related amyloid-β peptide formed oligomeric protofibrilar aggregates on the mica but elongated assembly on the HOPG (Kellermayer et al., 2008; Kowalewski and Holtzman, 1999), while the Parkinson's disease-related protein, α-synuclein, only formed sheet-like morphology on the mica, but not on the HOPG (Hoyer et al., 2004). These examples point out that the substrate-peptide interaction is critical but case sensitive in peptide assembly. Therefore, to summarize a general rule for elucidating how the substrate affects the peptide assembly structure and dynamics, sufficient data including the assembly of peptides with

*Correspondence to: Prof. Feng Zhang, School of Life Sciences, Inner Mongolia Agricultural University, 306 Zhaowuda Road, Inner Mongolia, Hohhot 010018, China. E-mail: fengzhang1978@imau.edu.cn (or) Prof. Yi Zhang, Shanghai Institute of Applied Physics, Chinese Academy of Sciences, 2019 Jialuo Road, Shanghai 201800, China. E-mail: zhangyi@sinap.ac.cn

Received 25 November 2014; accepted in revised form 14 February 2015

REVIEW EDITOR: Prof. Alberto Diaspro

Abbreviations: AFM, atomic force microscopy; HOPG, highly oriented pyrolytic graphite; HPLC, high performance liquid chromatography; MD, molecular dynamics; TEM, transmission electron microscopy; ThT, Thioflavin T.

Contract grant sponsor: National Basic Research Program of China; Contract grant number: 2013CB932801; Contract grant sponsor: National Natural Science Foundation of China; Contract grant numbers: 11274334, 21171086, 81160213; Contract grant sponsor: Inner Mongolia Grassland Talent; Contract grant number: 108–108038.

DOI 10.1002/jemt.22483
Published online 5 March 2015 in Wiley Online Library (wileyonlinelibrary.com).

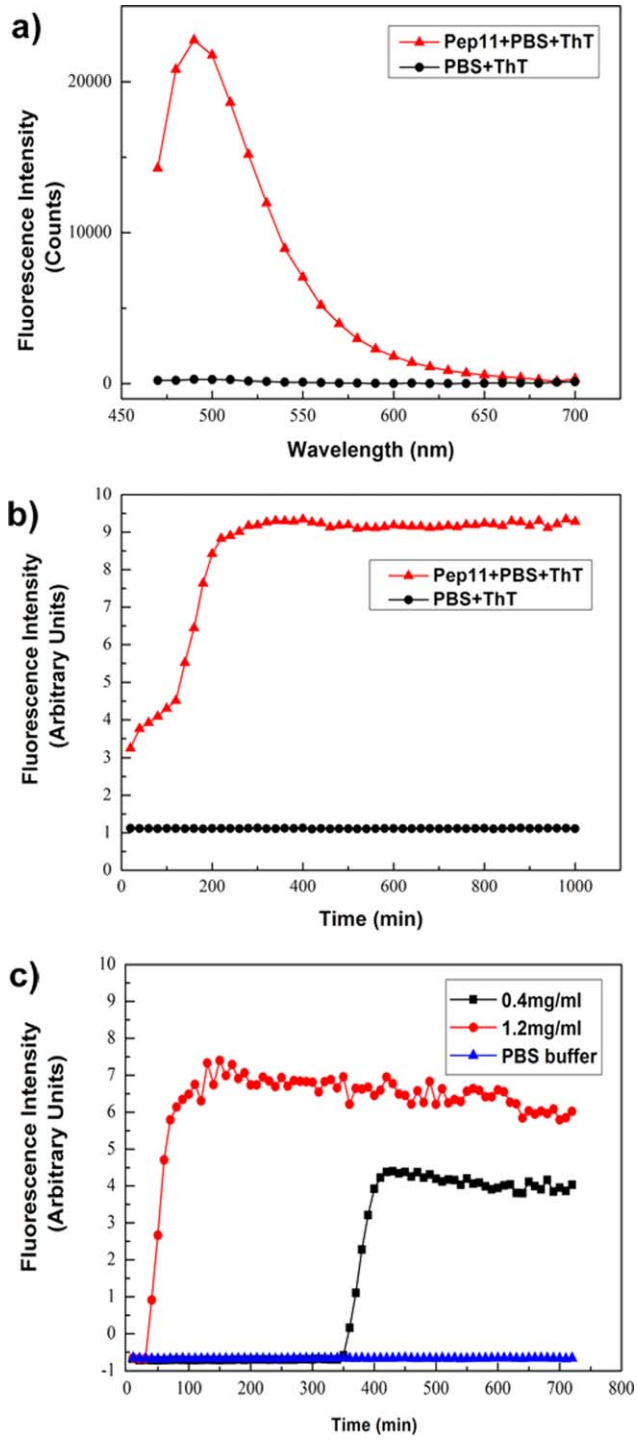

Fig. 1. The ThT fluorescence analysis during the assembly of Pep11. (**a**) ThT fluorescence shows maximum emission at 480∼490 nm in Pep11 solutions. The fluorescence of the Pep 11 solutions with a concentration of 0.8 mg/mL in 10 mM PBS buffer mixed with ThT (final concentration of 10 μM) was measured after incubation at 37°C for 5 h. (b–c) ThT fluorescence emission indicates the assembly kinetics of Pep11. Peptide concentration was 0.8 mg/mL (**b**), 1.2 mg/mL and 0.4 mg/mL (**c**), respectively, in 10 mM PBS buffer mixed with 10 μM ThT. The fluorescence in the Pep11 solutions was monitored during incubation at 37°C with constant agitation (900 rpm). The excitation wavelength was 440 nm. [Color figure can be viewed in the online issue, which is available at wileyonlinelibrary.com.]

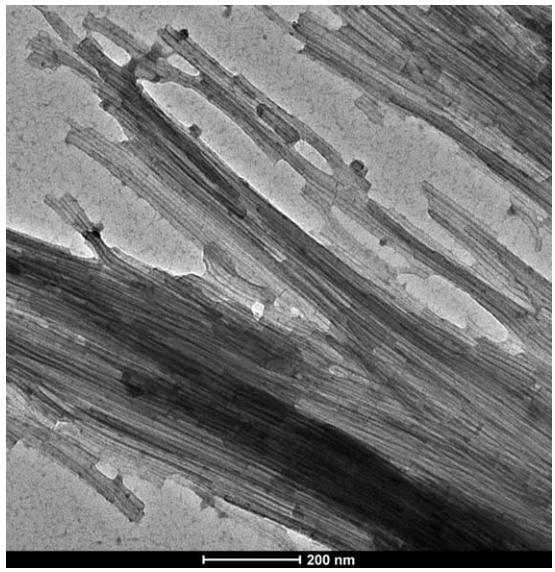

Fig. 2. A typical TEM image showing bundles of Pep11 filaments.

rationally designed sequences on model substrates should be collected.

In this article, we studied the interfacial effects on the self-assembly of an 11-residue model peptide. The peptide is originated from DN1 (or $P_{11}-2$, depending on different literatures), CH_3CO–Gln–Gln–Arg–Phe–Gln–Trp–Gln–Phe–Glu–Gln–Gln–NH_2, which was designed and first explored by Aggeli and co-workers (Aggeli et al., 1997). The DN1 peptide consists of two hydrophilic amino acid residuals (Arg and Glu), which can be oppositely charged and provide strong electrostatic interaction during peptide assembly. In addition, the aromatic amino acid residuals (Phe and Trp) in the sequence produce intermolecular recognition through π–π stacking. These designs in the sequence endow the DN1 peptide a favorite antiparallel alignment of the strands. Previous study showed that the DN1 peptide adopts a β-strand conformation in water and self-assembles into tape-like structures (Aggeli et al., 1997). Systematically studies indicated that the peptide and its relatives can hierarchically self-assemble into β-sheet tapes, ribbons, and fibers in bulk solutions (Aggeli et al., 2001, 2003). Although the DN1 serves a good model molecule for studying peptide self-assembly, very few reports (Whitehouse et al., 2005) regarding its self-assembly on solid substrates were available.

Previous studies showed that hydrophilic and hydrophobic substrates have quite different effects on the formation of peptide nanofilaments (Giacomelli and Norde, 2005; Kowalewski and Holtzman, 1999; Lashuel et al., 2000; Sherratt et al., 2004; Zhang et al., 2006). In this study we use mica and HOPG as model substrates to study the surface effects on the self-assembly behaviors of the N-terminal-deacetylated DN1, termed Pep 11 (NH_2–Gln–Gln–Arg–Phe–Gln–Trp–Gln–Phe–Glu–Gln–Gln–NH_2), and compared with its self-assembly behaviors in bulk solutions. It was found that Pep11 peptide assembled into amyloid-like filaments in bulk water solutions as revealed by

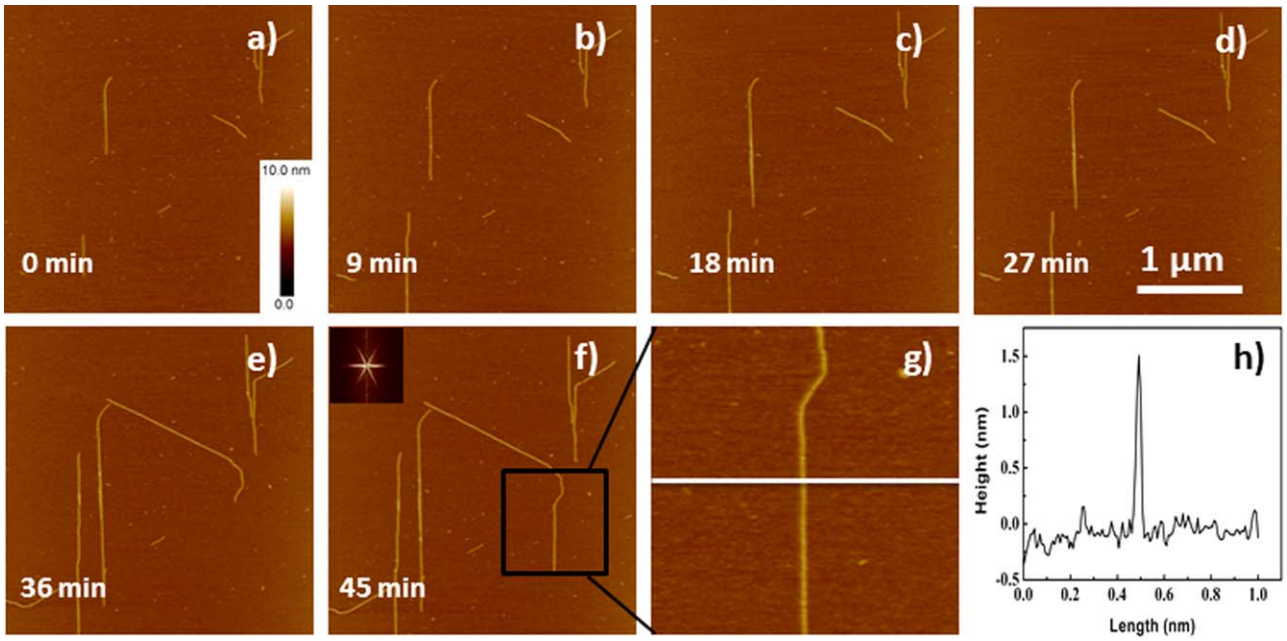

Fig. 3. (**a–f**) In situ AFM observation of Pep11 filaments growing on mica. The peptide concentration was 0.4 mg/mL in 10 mM PBS buffer. The time interval, from sample injecting into the liquid cell to successfully collecting AFM image, was labeled in each image. Inset in (f) shows the Fourier transform of the image. The Z scale bar shown in (a) and X–Y scale bar in (d) apply to images (a–f). (**g**) A zoom-in AFM image (1 μm × 1 μm) of Pep11 filaments formed on the mica substrate. (**h**) Section analysis of the line marked in g) indicating a height of ~1.5 nm for the peptide filament. [Color figure can be viewed in the online issue, which is available at wileyonlinelibrary.com.]

Thioflavin T (ThT) fluorescence analysis and transmission electron microscopy (TEM) morphology study. On the mica substrate, AFM in situ observation indicated that Pep11 assembled into one-dimensional filaments with a thickness of 1.5 nm. On HOPG, AFM study revealed that the peptide always assembled into well-defined ordered filaments with a thickness of 1 nm. These results emphasize the effects of substrates on modulating the assembled peptide features.

MATERIALS AND METHODS

Chemicals

The peptide Pep11 (NH_2-QQEFQWQFRQQ-$CONH_2$) was custom-synthesized from China Peptides. The sample had a purity of 98.3%, which was verified by high performance liquid chromatography (HPLC), and was further characterized with mass spectrum. The lyophilized powder was stored at −20°C. Before used, the peptide powder was dissolved in 10 mM PBS buffer (Phosphate 10 mM, NaCl 10 mM, pH 7.2) to a certain peptide concentration. Then the solutions were centrifuged with a rate of 10,000 rpm for 10 min to get rid of the possible aggregates, and the supernatant was immediately used or distributed in aliquots to different PE tubes and kept in the freezer (−20°C). Other chemicals were purchased from Sigma and used without further purification.

Atomic Force Microscopy (AFM)

All AFM images were obtained with a commercial AFM instrument (Nanoscope V, Veeco/Digital Instruments) equipped with a 100-μm scanner and a liquid cell. Experiments were performed in tapping mode under liquid. Silicon nitride cantilevers with a nominal spring constant of 0.35 N/m (SNL-10, Bruker) were used. All the images were taken at a resolution of 512 × 512 pixels. Muscovite mica [$KAl_2(Si_3Al)O_{10}(OH)_2$, Sichuan Meifeng, China] and HOPG (ZYB grade, NT-MDT, Moscow) were used as the inorganic substrates, which were freshly cleaved by adhesive tape before each experiment. After the as-prepared peptide solution was filled in the liquid cell, AFM imaging started immediately to study the dynamics of peptide assembly. AFM images were processed with Flatten function to remove any tilts during imaging and analyzed with the Offline software (NanoScope Analysis Version 1.40) that was supplied by the AFM manufacture.

ThT Fluorescence Analysis

The fibrosis of Pep11 was studied by monitoring the ThT fluorescence with an ELISA instrument (Gene Company Limited) or a Thermo Scientific Fluoroskan Ascent (ThermoFisherScientific, USA) at 37°C with a constant agitation (900 rpm). The concentrations of the peptide were 0.4, 0.8, and 1.2 mg/mL, respectively, in 10 mM PBS buffer.

Transmission Electron Microscopy (TEM)

Pep11 with a concentration of 0.8 mg/mL in 10 mM PBS buffer was incubated at 37°C with constant agitation (900 rpm) for 7 days. Then the samples were deposited on 400-mesh carbon TEM grids and stained with 0.75% uranyl formate. TEM images were obtained by using Tecnai G2 Spirit TEM operated at an accelerating voltage of 120 kV.

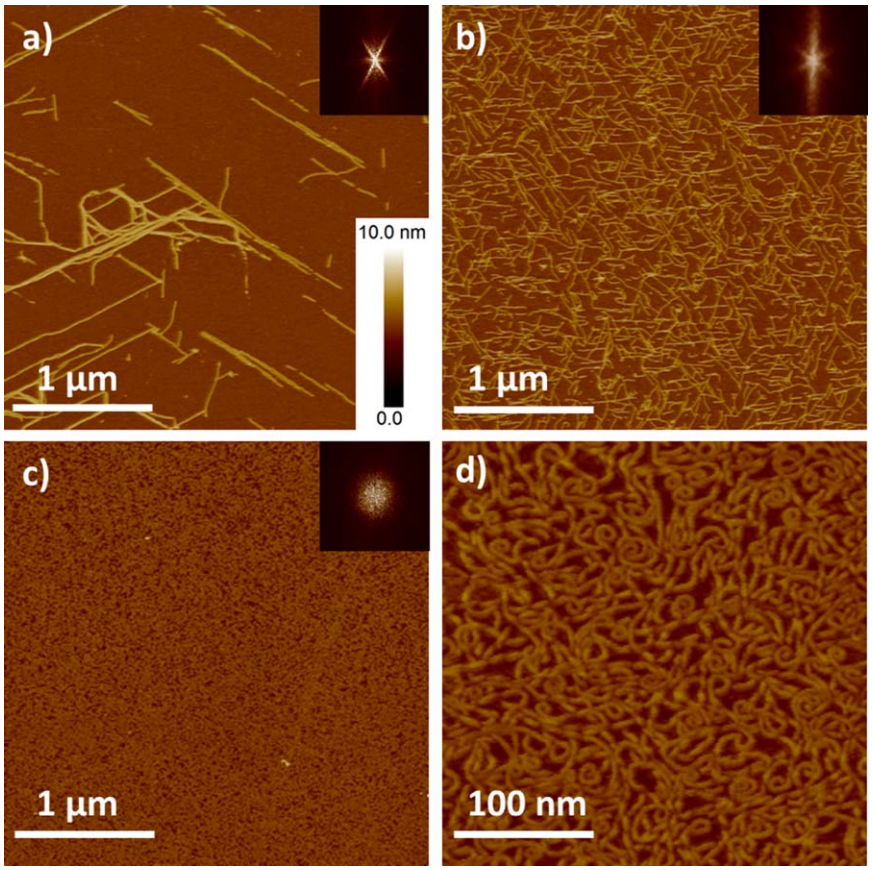

Fig. 4. AFM images showing Pep11 filaments after assembling for 50 min on mica with different peptide concentrations in 10 mM PBS buffer. (**a**) 0.6 mg/mL; (**b**) 0.8 mg/mL; (**c**, **d**) 1.2 mg/mL. Fourier transforms of the images (a) and (b) (see insets) indicated the filaments aligned with a hexagonal symmetry, while the Fourier transform of the image c (see inset) indicated the filaments were disordered. The Z scale bar shown in (a) applies to all images. [Color figure can be viewed in the online issue, which is available at wileyonlinelibrary.com.]

RESULTS AND DISCUSSION

It is well known that fluorescent molecule ThT specifically binds to amyloid fibrils having β-sheet structures, generating an emission around 482 nm (Bruinsma et al., 2011; Knowles and Buehler, 2011; LeVine, 1993). Therefore, it has been widely applied in studying the kinetics of amyloid fibril formation. Figure 1a is a typical ThT fluorescent emission spectrum, which shows an increasing fluorescence signal with a peak around 480–490 nm, indicating Pep11 formed amyloid-like β-sheet structures in the solutions. To study the kinetics of the peptide assembly, ThT fluorescence (emission wavelength of 480 nm) was monitored during incubation. As expected, the intensity of ThT fluorescence signals from Pep11 solutions remarkably enhanced with the increase of incubation time (Fig. 1b), though the signal was not very stable at the first 20 min. The fluorescent spectrum in Figure 1b can be roughly divided into three parts. During the first 120-min incubation, the fluorescence intensity increases in a slow rate, most possibly it was resulted from growth of the nucleation seeds of filaments in this stage. Then, a fast increasing of the fluorescence intensity was observed in the next 100-min incubation, indicating quick growth of the Pep11 amyloid-like filament structures. After that, the fluorescent intensity tends to stationary, and sustains tens of hours, suggesting that Pep11 in PBS can assemble into stable β-sheet structures. ThT fluorescence analysis was also conducted for the Pep11 peptide with concentrations of 1.2 and 0.4 mg/mL (in 10 mM PBS buffer mixed with 10 μM ThT), respectively. Results indicated that a longer incubating time was required for the peptide solution with a low concentration to reach the maximum fluorescent emittance (Fig. 1c).

TEM studies were carried out to visualize the Pep11 amyloid-like structures. Figure 2 shows a bundle of Pep11 filaments formed by incubating the Pep11 solutions (0.8 mg/mL peptide in 10 mM PBS buffer) at 37°C for 7 days with a constant agitation (900 rpm). The filament structures have a typical width of 10–20 nm, and can be as long as tens of micro. These results prove that Pep11 assembled into well-defined nanostructures in buck aqueous solutions.

The assembly properties of the Pep11 on mica substrate were investigated by using AFM in situ observation. After the peptide solution was injected into the liquid cell, AFM imaging was carried out immediately. It was found that the Pep11 self-assembled into

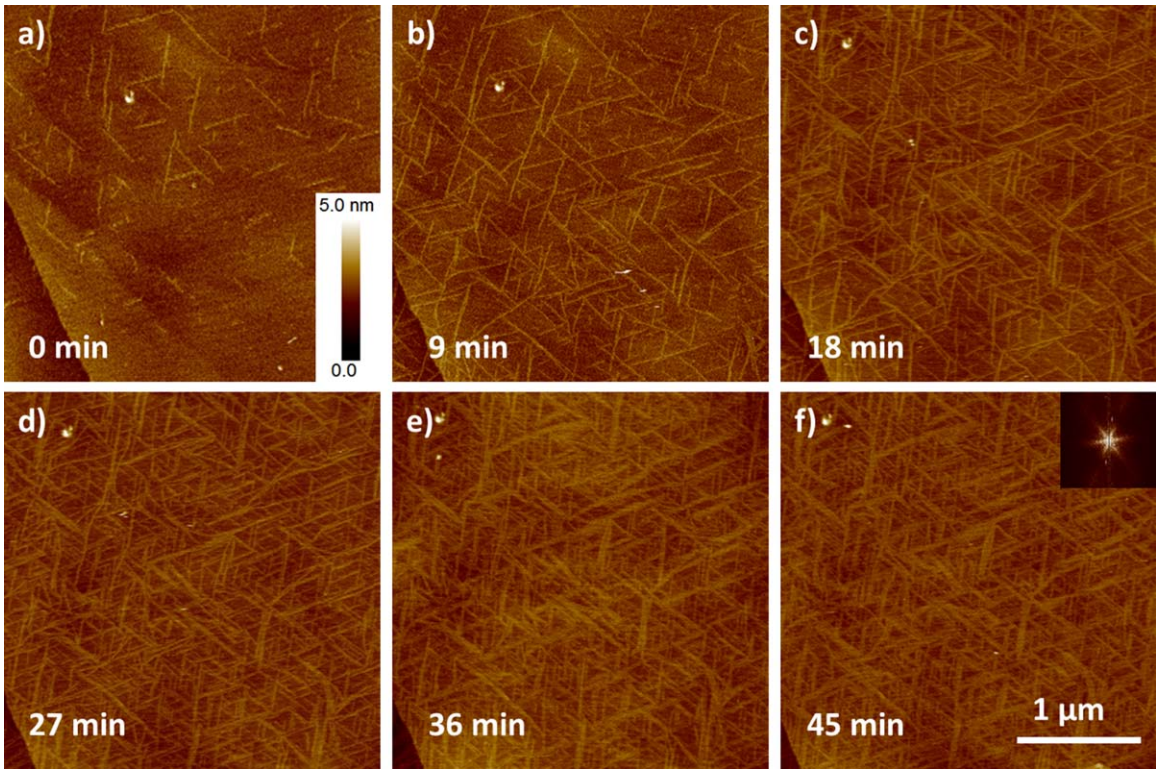

Fig. 5. (**a–f**) In situ AFM observation of Pep11 filaments growing on HOPG. The peptide concentration was 0.01 mg/mL in 10 mM PBS solutions. The time interval, from sample injecting into the liquid cell to successfully collecting AFM image, was labeled in each image. Inset in (f) is the Fourier transform of the image. The Z scale bar shown in (a) and X–Y scale bar in (f) apply to all images. [Color figure can be viewed in the online issue, which is available at wileyonlinelibrary.com.]

nanofilaments on mica substrate when its concentration reaches 0.4 mg/mL or higher. A series of images shown in Figure 3 are typical examples indicating the dynamic details of the peptide assembly. Normally, the filaments can grow bidirectionally and extend on the substrate to a length of several micrometers. The filaments never overlapped with each other and would stop growing when they encounter together. From the Fast Fourier Transform image (inset in Figure 3f), the growth of filaments showed three preferred orientations with an angle of 60° to each other, a direct sign of epitaxial growth process that is similar to those previously reported (Bittner, 2005; Brown et al., 2002; Ha and Park, 2005; Hoyer et al., 2004; Yang et al., 2002).

The one-dimensional epitaxial growth manner on mica substrate of the Pep11 is consistent with that of $P_{11}-2$. (Whitehouse et al., 2005) However, differences are also evident. First, Pep11 assembled under PBS buffer, while $P_{11}-2$ was unable to form assemblies on mica under aqueous solutions and had to use a 2-propanol–water (9:1) mixture as the solvent. The difference was attributed to the free NH_2- group in N-terminal of Pep11, which makes the molecule more hydrophilic. In addition, it can be positively charged under a neutral pH, which provides extra affinity to the mica substrate through the electrostatic interaction with the K^+ cavity of the substrate (Dai et al., 2013; Kang et al., 2013). Second, the Pep11 filament on mica has a height of 1.5 nm, according to AFM measurement. In contrast, the height of tape-like structures formed by $P_{11}-2$ on mica is 0.8 nm (Whitehouse et al., 2005), with which it is believed that the molecule is oriented flat on the substrate. We speculate that, under PBS buffer, water molecules may fill in the space between peptide and hydrophilic mica substrate. The hydrophilic amino acid residuals in the peptide may also stretch their side chains so that the positively charged Arg oriented close to substrate while the negatively charged Glu did oppositely. Both effects result in an elevated flat peptide assembly. However, it is also possible that the molecule partly take an "upright" conformation (Kang et al., 2013; Kang et al., 2012), or tilted upright orientation on the substrate so that the filament would be higher than the hydrodynamic diameter of a single molecule. Currently we are unable to precisely illustrate how the Pep11 molecules arrange in the filament on mica.

It was found that the assembly properties of Pep11 on mica are highly dependent on the peptide concentration. When the peptide concentration is less than 0.4 mg/ml, very little filaments could be found on the substrate. Peptide assembled on mica at an increasing rate along with the increase of the peptide concentration, as evidenced by the higher filament coverages on the substrates at higher concentrations in a same assembling time (Fig. 4). Another interesting phenomenon is the presence of randomly oriented filaments under higher peptide concentrations. In an extreme case, the filaments formed at a peptide concentration of 1.2 mg/mL were totally disordered and all in a

curved morphology (Figs. 4c and 4d). This result indicates that the assembly of Pep11 on mica is dominated with different rules under different peptide concentrations. In low peptide concentrations, it is a thermodynamically dependent process, so that the peptide filaments are aligned with the hexagonal symmetry of the underlying mica lattice to a lowest energy state. On the other hand, in high peptide concentrations (e.g. >1 mg/mL), the peptide assembles very quickly into filaments, and the assembly process is less influenced by the mica substrate.

The assembly of Pep11 was also conducted on the nonpolar HOPG substrate under PBS solutions. It is generally accepted that the hydrophobic interaction between substrate surface and the side chain of peptide is a primary driving force for the peptide assembly on HOPG (Kang et al., 2013; Kellermayer et al., 2008; Kowalewski and Holtzman, 1999). We think this is also the case for pep11 assembly on HOPG. It was found that, though several hydrophilic amino acid residuals presented in the sequence, the Pep11 assembled on HOPG very fast. To investigate the assembly process with in situ AFM imaging, peptide solutions has to be diluted. Figure 5 shows a typical process of formation and bidirectional extending of filaments with a peptide concentration of 0.01mg/mL in 10 mM PBS buffer, almost two magnitudes of order lower than that used in the assembly on mica. The filaments are all oriented in a well-defined manner, with an angle of 60° to each other, indicating it grew epitaxially and formed two-dimensional network that reflects the hexagonal symmetry of the underneath substrate. The filaments are normally shorter than several micrometers, since a filament with such a length would most likely encounter other ones and stop extending. All the filaments have a uniform height about 1 nm, indicating the molecules adopt "lying down" orientation on the substrate (Whitehouse et al., 2005; Zhang et al., 2006). These results suggest the Pep11 assembled with a different manner on HOPG than that on the mica substrate.

CONCLUSIONS

In summary, we have investigated the self-assembly of amyloid-like Pep11 both at water–solid interfaces and in bulk solutions. TEM imaging proved that Pep11 formed into filaments in bulk PBS solutions. The characteristic ThT fluorescent peak confirmed that the peptide was in β-sheet conformation in the solutions. AFM in situ observation showed that orderly arranged peptide filaments with three preferred orientations were formed immediately when the peptide solutions was added onto a mica / HOPG substrate. However, the ordered orientation of the peptide filament on mica only happened in low peptide concentrations, while the Pep11 filaments on HOPG were all oriented in a well-defined manner at any peptide concentrations. In addition, the kinetics in filament formation and the morphologies of the formed filaments either on HOPG and mica or in bulk solutions were quite different, indicating a highly dependence on the interfacial properties. Our study provides a full scenario of a model peptide assembling at interfaces, and should be helpful for understanding the assembly mechanism of amyloid-like peptides.

REFERENCES

Aggeli A, Bell M, Boden N, Keen JN, Knowles PF, McLeish TC, Pitkeathly M, Radford SE. 1997. Responsive gels formed by the spontaneous self-assembly of peptides into polymeric beta-sheet tapes. Nature 386:259–262.

Aggeli A, Bell M, Carrick LM, Fishwick CW, Harding R, Mawer PJ, Radford SE, Strong AE, Boden N. 2003. pH as a trigger of peptide beta-sheet self-assembly and reversible switching between nematic and isotropic phases. J Am Chem Soc 125:9619–9628.

Aggeli A, Nyrkova IA, Bell M, Harding R, Carrick L, McLeish TC, Semenov AN, Boden N. 2001. Hierarchical self-assembly of chiral rod-like molecules as a model for peptide beta -sheet tapes, ribbons, fibrils, and fibers. Proc Natl Acad Sci U S A 98:11857–11862.

Bittner AM. 2005. Biomolecular rods and tubes in nanotechnology. Naturwissenschaften 92:51–64.

Brown CL, Aksay IA, Saville DA, Hecht MH. 2002. Template-directed assembly of a de novo designed protein. J Am Chem Soc 124: 6846–6848.

Bruinsma IB, Karawajczyk A, Schaftenaar G, de Waal RMW, Verbeek MM, van Delft FL. 2011. A rational design to create hybrid beta-sheet breaker peptides to inhibit aggregation and toxicity of amyloid-beta. MedChemComm 2:60–64.

Butterfield SM, Lashuel HA. 2010. Amyloidogenic protein-membrane interactions: Mechanistic insight from model systems. Angew Chem Int Ed 49:5628–5654.

Cherny I, Gazit E. 2008. Amyloids: Not only pathological agents but also ordered nanomaterials. Angew Chem Int Ed 47: 4062–4069.

Chiti F, Dobson CM. 2006. Protein misfolding, functional amyloid, and human disease. Annu Rev Biochem 75:333–366.

Dai B, Kang SG, Huynh T, Lei H, Castelli M, Hu J, Zhang Y, Zhou R. 2013. Salts drive controllable multilayered upright assembly of amyloid-like peptides at mica/water interface. Proc Natl Acad Sci U S A 110:8543–8548.

Du HN, Tang L, Luo XY, Li HT, Hu J, Zhou JW, Hu HY. 2003. A peptide motif consisting of glycine, alanine, and valine is required for the fibrillization and cytotoxicity of human alpha-synuclein. Biochemistry 42:8870–8878.

Ellis-Behnke RG, Liang YX, You SW, Tay DK, Zhang S, So KF, Schneider GE. 2006. Nano neuro knitting: Peptide nanofiber scaffold for brain repair and axon regeneration with functional return of vision. Proc Natl Acad Sci U S A 103(13):5054–5059.

Giacomelli CE, Norde W. 2005. Conformational changes of the amyloid beta-peptide (1–40) adsorbed on solid surfaces. Macromol Biosci 5:401–407.

Ha C, Park CB. 2005. Template-directed self-assembly and growth of insulin amyloid fibrils. Biotechnol Bioeng 90:848–855.

Hoyer W, Cherny D, Subramaniam V, Jovin TM. 2004. Rapid self-assembly of alpha-synuclein observed by in situ atomic force microscopy. J Mol Biol 340:127–139.

Kang SG, Huynh T, Xia Z, Zhang Y, Fang H, Wei G, Zhou R. 2013. Hydrophobic interaction drives surface-assisted epitaxial assembly of amyloid-like peptides. J Am Chem Soc 135:3150–3157.

Kang SG, Li H, Huynh T, Zhang F, Xia Z, Zhang Y, Zhou R. 2012. Molecular mechanism of surface-assisted epitaxial self-assembly of amyloid-like peptides. ACS Nano 6:9276–9282.

Kellermayer MS, Karsai A, Benke M, Soos K, Penke B. 2008. Stepwise dynamics of epitaxially growing single amyloid fibrils. Proc Natl Acad Sci U S A 105:141–144.

Knowles TP, Buehler MJ. 2011. Nanomechanics of functional and pathological amyloid materials. Nat Nanotechnol 6:469–479.

Kowalewski T, Holtzman DM. 1999. In situ atomic force microscopy study of Alzheimer's beta-amyloid peptide on different substrates: New insights into mechanism of beta-sheet formation. Proc Natl Acad Sci U S A 96:3688–3693.

Lashuel HA, Labrenz SR, Woo L, Serpell LC, Kelly JW. 2000. Protofilaments, filaments, ribbons, and fibrils from peptidomimetic self-assembly: Implications for amyloid fibril formation and materials science. J Am Chem Soc 122:5262–5277.

LeVine H, III. 1993. Thioflavine T interaction with synthetic Alzheimer's disease beta-amyloid peptides: Detection of amyloid aggregation in solution. Protein Sci 2:404–410.

Li D, Furukawa H, Deng H, Liu C, Yaghi OM, Eisenberg DS. 2014. Designed amyloid fibers as materials for selective carbon dioxide capture. Proc Natl Acad Sci U S A 111:191–196.

Lim YB, Lee E, Lee M. 2007. Cell-penetrating-peptide-coated nanoribbons for intracellular nanocarriers. Angew Chem Int Ed 46: 3475–3478.

Mao XB, Wang CX, Wu XK, Ma XJ, Liu L, Zhang L, Niu L, Guo YY, Li DH, Yang YL, Wang C. 2011. Beta structure motifs of islet amyloid

polypeptides identified through surface-mediated assemblies. Proc Natl Acad Sci U S A 108:19605–19610.
Murphy RM. 2007. Kinetics of amyloid formation and membrane interaction with amyloidogenic proteins. Biochim Biophys Acta 1768:1923–1934.
Reches M, Gazit E. 2003. Casting metal nanowires within discrete self-assembled peptide nanotubes. Science 300:625–627.
Rufo CM, Moroz YS, Moroz OV, Stohr J, Smith TA, Hu X, DeGrado WF, Korendovych IV. 2014. Short peptides self-assemble to produce catalytic amyloids. Nat Chem 6:303–309.
Ryadnov MG, Ceyhan B, Niemeyer CM, Woolfson DN. 2003. "Belt and braces": A peptide-based linker system of de novo design. J Am Chem Soc 125:9388–9394.
Sherratt MJ, Holmes DF, Shuttleworth CA, Kielty CM. 2004. Substrate-dependent morphology of supramolecular assemblies: Fibrillin and type-VI collagen microfibrils. Biophys J 86:3211–3222.
Vauthey S, Santoso S, Gong H, Watson N, Zhang S. 2002. Molecular self-assembly of surfactant-like peptides to form nanotubes and nanovesicles. Proc Natl Acad Sci U S A 99:5355–5360.
Wagner DE, Phillips CL, Ali WM, Nybakken GE, Crawford ED, Schwab AD, Smith WF, Fairman R. 2005. Toward the development of peptide nanofilaments and nanoropes as smart materials. Proc Natl Acad Sci U S A 102:12656–12661.
Whitehouse C, Fang J, Aggeli A, Bell M, Brydson R, Fishwick CW, Henderson JR, Knobler CM, Owens RW, Thomson NH, Smith DA, Boden N. 2005. Adsorption and self-assembly of peptides on mica substrates. Angew Chem Int Ed 44:1965–1968.
Yang G, Woodhouse KA, Yip CM. 2002. Substrate-facilitated assembly of elastin-like peptides: Studies by variable-temperature in situ atomic force microscopy. J Am Chem Soc 124:10648–10649.
Yang H, Fung SY, Pritzker M, Chen P. 2009. Ionic-complementary peptide matrix for enzyme immobilization and biomolecular sensing. Langmuir 25:7773–7777.
Yemini M, Reches M, Rishpon J, Gazit E. 2005. Novel electrochemical biosensing platform using self-assembled peptide nanotubes. Nano Lett 5:183–186.
Yokoi H, Kinoshita T, Zhang S. 2005. Dynamic reassembly of peptide RADA16 nanofiber scaffold. Proc Natl Acad Sci U S A 102:8414–8419.
Yolamanova M, Meier C, Shaytan AK, Vas V, Bertoncini CW, Arnold F, Zirafi O, Usmani SM, Muller JA, Sauter D, Goffinet C, Palesch D, Walther P, Roan NR, Geiger H, Lunov O, Simmet T, Bohne J, Schrezenmeier H, Schwarz K, Standker L, Forssmann WG, Salvatella X, Khalatur PG, Khokhlov AR, Knowles TP, Weil T, Kirchhoff F, Munch J. 2013. Peptide nanofibrils boost retroviral gene transfer and provide a rapid means for concentrating viruses. Nat Nanotechnol 8:130–136.
Zhang F, Du HN, Zhang ZX, Ji LN, Li HT, Tang L, Wang HB, Fan CH, Xu HJ, Zhang Y, Hu J, Hu HY, He JH. 2006. Epitaxial growth of peptide nanofilaments on inorganic surfaces: Effects of interfacial hydrophobicity/hydrophilicity. Angew Chem Int Ed 45:3611–3613.
Zhu M, Souillac PO, Ionescu-Zanetti C, Carter SA, Fink AL. 2002. Surface-catalyzed amyloid fibril formation. J Bio Chem 277:50914–50922.